A physically-based climatology of Australian east coast lows occurrence and intensification

Leone Cavicchia*

School of Earth Sciences, The University of Melbourne, Melbourne, Australia

Acacia Pepler

Bureau of Meteorology, Sydney, Australia

Andrew Dowdy

Bureau of Meteorology, Melbourne, Australia

Kevin Walsh

School of Earth Sciences, The University of Melbourne, Melbourne, Australia

Corresponding author address: School of Earth Sciences, The University of Melbourne, 3010 Victoria, Australia.

E-mail: leone.cavicchia@unimelb.edu.au

ABSTRACT

The subtropical part of the eastern Australian seaboard experiences intense cyclonic activity. The severe damage caused by the intense storms in the region, known as east coast lows (ECLs), has motivated a number of recent studies. Cyclones in this region appear to be driven by a combination of different (barotropic and baroclinic) formation mechanisms, consistent with the view emerging in the last decades that cyclones span a continuous spectrum of dynamical structures, with the barotropically driven tropical cyclone and the baroclinically driven extra-tropical cyclone being only the extremes of such spectrum. In this work we revisit the climatology of cyclone occurrence in the subtropical east coast of Australia as seen in a global reanalysis, systematically applying classification criteria based on the cyclone vertical structure and thermal core. Moreover, we investigate the underlying processes driving the cyclone rapid intensification by means of an atmospheric limited area energetics analysis. We show that ECLs have different spatial patterns according to the cyclone thermal structure, with the fraction of hybrid cyclones being larger towards the tropics and closer to the coast. Moreover, we find that explosively deepening cyclones in this region are driven by a different combination of processes with respect to the global case, with barotropic processes in the surrounding environment having a more dominant role in the energetics of cyclone rapid intensification. The findings of this work contribute to understanding the physical processes underlying the formation and intensification of Australian east coast lows and the associated coastal damage and risk.

1. Introduction

The portion of the east coast of Australia extending between the subtropics and the mid-latitudes (the area corresponding approximately to the latitudes between 25° S to 40° S and the longitudes between 150° E and 160° E) experiences a frequent occurrence of intense low pressure systems. This type of cyclones is generally known as east coast lows (ECLs). Such systems can occur year-round; the most intense events, however, are normally observed during the transition to the cold season (Hopkins and Holland 1997). Strong ECLs can cause severe damage - associated with heavy rain, strong winds, and storm surge - when they hit highly populated areas along the southeast Australian coast, where a large part of the country's population and economic activities are based (e.g., more than two thirds of Australia's population live within 50 km of the continent's eastern seaboard[1]). One such low pressure system occurred in 2007 and is ranked among the ten worst natural disasters in Australia in terms of insured losses[2]. Extreme weather associated with this system, known as the Pasha Bulker ECL, was recorded, including peak wind gust up to 36 m/s, flash flooding with rainfall of 466 mm, and major coastal erosion with 14 m maximum wave heights (Mills et al. 2010).

East coast lows have a spatial scale ranging from synoptic to mesoscale (100 to 1000 km), and often have a rapid development including during the night. However, some ECL properties can vary significantly depending on the definition adopted. The frequency can vary from one or two per year if only intense events producing severe impact on the coast are considered (Holland et al. 1987), to about twenty per year when all identified low pressure systems in the region are included (Speer et al. 2009).

[1]Source: Australian Bureau of Statistics http://www.abs.gov.au/ausstats/abs@.nsf/Previousproducts/1301.0Feature%20Article32004

[2]Source: Insurance Council of Australia, http://www.icadataglobe.com/access-catastrophe-data/

The first studies of the properties of Australian ECLs cases date back to the 1950s (Kraus 1954; Clarke 1956), with later studies focusing on producing climatologies of storm occurrence and classifying their synoptic environments (Holland et al. 1987; Hopkins and Holland 1997). The last decade has seen a renewed interest in studies aimed at building climatologies of the occurrence of ECLs based on the increasing availability of higher resolution reanalysis and modeling datasets. Speer et al. (2009) provided a new long-term database of ECL events, compiled by visually identifying low pressure events in sea level pressure charts, and this approach has been commonly used to date as the best estimate of the observed frequency of ECLs. Other studies have focused on objective identification methods, typically based on the application of an automated detection scheme to one or more reanalysis datasets. A number of works produced cyclone climatologies by applying different identification criteria, e.g. based on the Laplacian of sea level pressure (Pepler and Coutts-Smith 2013), sea level pressure gradients (Browning and Goodwin 2013), or upper level geostrophic vorticity (Dowdy et al. 2013). Recent studies focused on comparing the various tracking methods (Pepler et al. 2015) as well as the sources of climatological data (Di Luca et al. 2015). They concluded that while the agreement between studies on the frequency and properties of stronger storms is generally good, a larger sensitivity to the data and methods employed emerges when the smaller and/or weaker cyclones are taken into account.

A number of studies have investigated the dynamical nature of Australian ECLs. Previous works focusing on case studies of historical ECLs have shown that the broad ECL set contains both extra-tropical frontal storms and hybrid cyclones with mixed tropical/extra-tropical features (Garde et al. 2010; Mills et al. 2010; Cavicchia et al. 2018). This is consistent with the modern view (Hart 2003) that cyclones can span a continuous spectrum of dynamical structures, of which the completely barotropic tropical cyclone and the completely baroclinic extra-tropical cyclone only represent the extremes. At a regional scale, the occurrence of cyclones with hybrid tropical extratropi-

cal features has been documented in many different regions, including the southwestern Atlantic (Evans and Braun 2012; Gozzo et al. 2014), the northern Atlantic (Guishard et al. 2009; Mauk and Hobgood 2012; González-Alemán et al. 2015), the central North Pacific (Otkin and Martin 2004; Caruso and Businger 2006) and the Mediterranean Sea (Miglietta et al. 2013; Cavicchia et al. 2014; Walsh et al. 2014). At a global scale, modern cyclone climatologies indicate indeed that low pressure systems of differing dynamical nature typically coexist in the subtropical latitude belts of both hemispheres (from approximately 20° to 40°) and in particular on the continents' eastern seaboards (Yanase et al. 2014). In the ECL region, the vertical structure of a subset of cyclones was analyzed by Browning and Goodwin (2013) who presented a synoptic climatology of ECLs using a classification system based on genesis locations and tracks. They also employed the Hart (2003) phase space analysis to differentiate between cold core, hybrid and warm core structures.

Even though it has been known for a long time that cyclones affecting the east coast of Australia differ in their dynamical nature, the analysis of cyclone structure has been applied in previous studies as an *a posteriori* diagnostic applied to selected subsets of cyclones identified according to different criteria. However, in order to investigate the relative occurrence of different types of cyclones, and to what extent their properties (e.g., their distribution in space and time) differ according to the cyclone dynamical structure, the analysis of the structure of the storms would need to be applied systematically (i.e., irrespective of their other characteristics such as track and location in contrast to previous studies). The main goal of the present work is to close this knowledge gap, by systematically quantifying the climatological patterns of occurrence of low pressure systems in the east Australia coastal region according to cyclone structure, as described in terms of the vertical symmetry and thermal core. The classification of cyclones according to their structure is thus not aimed at replacing previous climatologies based on different classification criteria, but rather at better quantifying the occurrence of cyclones with different thermal structures. The

ultimate purpose of the new classification is an improvement in the understanding of the coastal damage and risk associated to those extreme weather events, according to their structure.

In terms of impact assessment, the interest is generally focused on the subset of cyclones that are likely to cause greater damage, depending on the affected area. Among the different metrics that have been developed to quantify the intensity of extratropical cyclones, the "bomb cyclone", defined by an "explosive intensification" criterion (Sanders and Gyakum 1980) has often been used to quantify the potential impacts of a storm. Such a criterion is based on the definition of a threshold characterizing the cyclone's rapid deepening (24 hPa in 24 hours at a latitude of 60 degrees). Studies of global occurrence of explosively intensifying cyclones (Allen et al. 2010; Lim and Simmonds 2002) have shown that the east coast of Australia is one of the areas where this kind of cyclone evolution is common. Black and Pezza (2013) showed, globally, that statistically robust signatures of the leading role of baroclinic processes emerge in the analysis of the energy cycle of explosively deepening cyclones. The second major goal of the present work is the systematic study of the energetics of explosively deepening versus non-rapidly deepening Australian ECLs, aimed at an improved understanding of the atmospheric processes underlying rapid intensification of cyclones. The analysis of cyclone energetics will be performed taking into account the separation of cyclones into different classes. Such a combined analysis of the energetics and cyclone classification is to our knowledge performed here for the first time for a multi-decadal cyclone climatology.

Summarizing, the present work aims at addressing a number of knowledge gaps in the understanding of Australian ECLs occurrence. This goal is pursued by exploiting two physically-based diagnostics aimed at classifying low pressure systems and investigating the mechanisms underlying their intensification. Such an approach has been tested for a number of test cases in previous work (Cavicchia et al. 2018), but it is here applied systematically to a multi-decadal dataset. In

particular, two main objectives were set for this study, addressing the following scientific questions:

1. The east coast of Australia has been shown to be affected by cyclones differing in their dynamical nature, ranging from transitioning tropical cyclones to extra-tropical cyclones with hybrid cyclones in between. What is the relative rate of occurrence of different types of cyclones? How do the statistical properties of cyclones, such as their distribution in space and time, differ according to their dynamical class? This question is addressed by classifying low pressure systems employing the cyclone phase space diagnostics.

2. What is the role of different barotropic and baroclinic physical processes in the intensification of different classes of cyclones? Does the large scale environment energetics provide a measure for ECLs' rapid intensification? In order to address this question the energetics cycles of explosively deepening cyclones with different thermal structures are analyzed and contrasted with non-rapidly intensifying cyclones.

Answering those questions is intended to provide a framework to investigate the coastal damage and risk associated with ECL occurrence, by improving the understanding the physical mechanisms underlying cyclone formation and intensification.

The rest of the manuscript is organized as follows. In Section 2, the data and methods used in this work are described. In Section 3, the results of the classification and energetics analysis of Australian ECLs are presented and discussed in detail. Finally, in Section 4, the main results of the present work are summarized and the most promising directions for future work are indicated.

2. Data and methods

a. Data

The atmospheric dataset used in this work is the ERA-Interim reanalysis (Dee et al. 2011), covering a 38-year period from 1979 to 2016. The ERA-Interim reanalysis data is available at 6-hourly frequency on a horizontal grid with a resolution of 0.75 degrees, and on 37 vertical pressure levels. Several studies have investigated the skill of this reanalysis in reproducing observed cyclone climatologies, including tropical cyclones (e.g. Hodges et al. (2017) and references therein), extratropical cyclones (e.g. Hodges et al. (2011) and references therein) as well other low pressure systems such as polar lows (Zappa et al. 2014). These studies concluded that ERA-Interim is generally able to reproduce the observed occurrence of cyclones. Depending on the type of analyzed low pressure systems, larger deviations can be found for some of the cyclone features such as intensity, with horizontal resolution being a critical factor for smaller scale systems (Simmonds et al. 2008; Pinto et al. 2005). In particular, several studies showed, for both tropical (Hodges et al. 2017) and extra-tropical cyclones (Hewson and Neu 2015), that ERA-Interim can underestimate cyclone central pressures up to around 10 hPa. Such underestimation can result in an uncertainty in diagnostics derived from cyclone pressure, such as the rate of explosive deepening; on the other hand, it was shown that the number of explosively deepening cyclones increase in ERA-Interim with respect to other reanalysis datasets, due to a better representation of smaller storms (Allen et al. 2010).

In previous studies objective climatologies of ECLs were created based on ERA-Interim, applying automated tracking and detection algorithms. The advantage of such climatologies with respect to previous catalogs of events such as the reference database of Speer et al. (2009) is that they don't rely on the visual inspection of pressure charts. Some of the statistical properties of

ERA-Interim generated ECL climatologies have been analyzed in Di Luca et al. (2015), showing that there is a good agreement between the cyclones detected in ERA-Interim and the ones in the reference database (Speer et al. 2009) for cyclone frequency, as well as their seasonal, inter-annual and spatial variability. A relatively larger sensitivity to resolution was found for summer cyclones, attributed to the larger fraction of smaller-scale low pressure systems in the warm season. Pepler et al. (2017) analyzed the wind and precipitation fields associated with a number of past ECL events in several reanalysis datasets, and found that ERA-Interim exhibits the highest degree of consistency with satellite wind and rainfall observations. A recent study (Cavicchia et al. 2018) looked at two recent ECL test cases examining properties similar to the ones investigated in the present study, such as cyclone phase space and energetics parameters, and found that there is a good agreement between ERA-Interim and higher-resolution datasets, obtained through dynamical downscaling, in the representation of these properties.

b. ECL definition

ECL are generally defined as closed low pressure systems occurring in a region extending few hundred kilometers from the coast in a latitude band between 20° S and 40° S. Additional criteria have been adopted in different ECL definitions and classification schemes in the literature. Some studies applied additional criteria based on the storm motion or location. For example, the Public Works Department (PWD) (1985) considered five different types of ECLs based on criteria such as the southward or northward direction of motion, the location relative to the Great Dividing Range, as well as whether the storm is located mostly over land or sea. Another example is the study of Holland et al. (1987), where three different types of ECLs were considered based on the location relative to some typical synoptic configurations in the area. Some studies use the term ECL for the subset of events causing severe impacts on coastal areas only, with examples of studies applying

definitions based on both the storm motion and impacts including Hopkins and Holland (1997) who defined a cyclone as an ECL if it had a motion parallel to the coast and was also associated with heavy rain.

Another type of ECL definition, on the other hand, is based on pressure criteria only including all low pressure systems occurring off the east coast of Australia applying pressure based thresholds to exclude very weak systems. In this work, we follow the latter approach. Following Pepler et al. (2015), ECLs are defined in this work as all the cyclones, subject to the sea level pressure thresholds defined in the objective cyclone tracking and detection scheme described in Section 2.c below, entering the ECL region shown in Fig. 3 for at least one six-hourly reanalysis time step.

c. Cyclone tracking scheme

Several automated schemes for the objective detection and tracking of cyclones in climate gridded datasets are available. They are usually based on either pressure variables or vorticity, or a combination of both. Several studies (e.g Neu et al. (2013), Raible et al. (2008)) showed that cyclone climatologies exhibit a sensitivity to the chosen tracking scheme, introducing a further source of variability additional to that arising from the choice of data source and resolution. Pepler et al. (2015) extensively compared several automated cyclone detection methods in the ECL region, testing different sets of detection parameters and found that good skill is shown by the pressure Laplacian-based University of Melbourne (UoM) detection scheme (Simmonds et al. 1999), when its parameters are tuned to optimize ECL detection to match the observational dataset of (Speer et al. 2009). While different representations of ECL activity exist, this particular dataset is based on a similar definition of an ECL to the one adopted in Pepler et al. (2015) and in the present work, and thus is well suited as a benchmark for the detection scheme. The UoM scheme has an advantage with respect to other methods with comparable skill at identifying ECLs, such as the

upper level geostrophic vorticity method of Dowdy et al. (2013) in applications where accurate information on storm location is needed based on surface pressure. In the present study, the UoM detection scheme is thus employed to track ECLs based on mean sea level pressure. The main features of the UoM scheme are described in the following paragraph, while further details can be found in Murray and Simmonds (1991), Simmonds et al. (1999).

The UoM scheme is based on the Laplacian of sea level pressure. The scheme is defined on a polar stereographic grid, thus the input fields have to be re-gridded to this grid, with a user-defined grid resolution. In the present work, a resolution of 1 degree is chosen following Pepler et al. (2015). The algorithm looks for local maxima of the Laplacian of sea level pressure ($\nabla^2 p$), and associates the cyclone location with a nearby closed pressure surface center. If an associated closed center is not found, the cyclone is classified as an open depression. In order to avoid detecting too many weak disturbances, a minimum value of $\nabla^2 p$ can be selected. In the present work the value is $(\nabla^2 p)_{min} = 1 hPa/^{\circ} lat$ following Pepler et al. (2015). Further adjustments to avoid the detection of too many spurious lows include the smoothing of the pressure field and the introduction of an orography-dependent corrective term in the Laplacian. Once the low pressure centers are identified, tracking is performed by predicting the subsequent low position according to the steering velocity (proportional to the 500 hPa wind), then assigning the detected pressure minimum at the next time step to the track according to the probability of a match between predicted and detected positions. If more than one suitable pressure minimum is found, the one that maximized the probability function is chosen.

The full tracking procedure consists of two steps. In the first step, cyclone tracks are detected globally using the algorithm described above. In the second step, the tracks that have a closed pressure center lying for at least one time step within the area depicted in Fig. 3, and that reach for

at least one time step a threshold value of the mean sea level pressure Laplacian $\nabla^2 p > 2.5 hPa/^\circ lat$ (in order to exclude weak systems) are selected and retained for further analysis.

d. Cyclone phase space

The cyclone phase space (CPS) diagnostics, originally developed by Hart (2003), are used in this work to classify cyclones. CPS was originally developed as a tool to study extra-tropical transitions of tropical cyclones. It is based on the idea that a limited number of variables can be identified, whose values have a well-defined threshold that allows separation of vertically-symmetric warm-cored tropical cyclones from vertically tilted cold-cored extra-tropical cyclones. Computing those variables for all the time steps where data is available, it is possible to follow the evolution of the storm dynamical structure during its lifetime. The CPS analysis is naturally well suited to also identify those cyclones that have a hybrid structure with mixed features, such as a partial warm core: CPS has therefore been used in several studies to study subtropical/hybrid cyclones (Yanase et al. 2014). The information on the cyclone dynamical features given by CPS, such as the vertical symmetry and thermal core, is useful to better understand the cyclone evolution and its implications in terms of coastal impacts.

CPS is based on three variables. One variable, the B parameter, indicates whether the vertical structure of the cyclone is symmetric or tilted. The other variables, V_T^L and V_T^U, quantify the thermal anomaly in the cyclone core with respect to the environment, indicating whether the cyclone is warm-cored or cold-cored. The two variables differ in taking into account different layers of the atmosphere. Figure 1 shows a schematic representation of the different features of cyclones in the CPS variable space.

All the variables can be computed from the three-dimensional geopotential field. The B parameter is defined as the difference between the thickness of the geopotential layer between 900 hPa

and 600 hPa averaged over two semicircles located to the left and to the right with respect to the direction of the storm motion:

$$B = \pm \left(\overline{Z|_{600hPa} - Z|_{900hPa}}\Big|_R - \overline{Z|_{600hPa} - Z|_{900hPa}}\Big|_L \right),$$

where the plus sign is applied in the northern hemisphere and the minus sign in the southern hemisphere. An absolute value of $B < 10$ indicates a symmetric cyclone, while $B > 10$ corresponds to a vertically-tilted cyclone.

The thermal wind parameters for the lower troposphere, V_T^L, and upper troposphere, V_T^U, are defined as the vertical derivative between 900 hPa and 600 hPa of the height gradient in a 500 km radius:

$$-V_T^L = \frac{\partial \left(Z_{max} - Z_{min}\right)|_{500km}}{\partial \ln p}\Bigg|_{600hPa}^{900hPa} \quad (1)$$

$$-V_T^U = \frac{\partial \left(Z_{max} - Z_{min}\right)|_{500km}}{\partial \ln p}\Bigg|_{300hPa}^{600hPa}, \quad (2)$$

where the vertical derivative is calculated from a linear regression fit of the height difference. A value of $-V_T^{L(U)} > 0$ indicates a warm-cored cyclone in the lower (upper) troposphere, i.e. a positive temperature anomaly in the cyclone core with respect to the surrounding environment. A value of $-V_T^{L(U)} < 0$, on the other hand, indicates a cold-cored cyclone in the lower (upper) troposphere, i.e. a negative temperature anomaly in the cyclone core with respect to the surrounding environment.

Throughout this work, three classes of cyclones are defined based on the thermal wind parameters V_T^U and V_T^L only: the cold-cored cyclone is associated with $-V_T^L < 0$ and $-V_T^U < 0$, warm-cored cyclone with $-V_T^L > 0$ and $-V_T^U > 0$ and the hybrid cyclone with $-V_T^L > 0$ and $-V_T^U < 0$.

e. Cyclone energetics

The limited area energetics is a framework that extends the partitioning of the atmosphere in the zonal and eddy components of available potential and kinetic energies (Lorenz 1955) to a limited domain in the atmosphere (Smith 1969; Johnson 1970) in order to study the processes that drive the energetics of severe weather systems such as cyclones (Michaelides 1987, 1992).

A schematic view of the limited area energetics framework is presented in Fig. 2. Similarly to the global energetics, the zonal (A_Z) and eddy (A_E) available potential energy terms are represented on the left part of the graph together with their respective generation terms (G_Z and G_E). On the other hand, on the right hand side of the graph the zonal (K_Z) and eddy (K_E) kinetic energy terms are shown together with their respective dissipation terms (D_Z and D_E). In a limited area domain, boundary terms contributing to each of the four energy terms have to be taken into account (respectively BA_Z, BA_E, BK_Z and BK_E). The energy conversion terms represent the transitions between the different energy forms: C_A is the conversion of zonal available potential energy into/from eddy available potential energy, C_E is the conversion of eddy available potential energy into/from eddy kinetic energy, C_Z is the conversion of zonal available potential energy into/from zonal kinetic energy, and C_K is the conversion of zonal kinetic energy into/from eddy kinetic energy. The different terms were computed following the procedure described in Veiga and Ambrizzi (2013), to which the reader is referred for the full details of the formal aspects of the computation. We summarize here, however, the physical interpretation according to Veiga and Ambrizzi (2013) of the terms of the energetics analysis that are more relevant when applied to investigate low pressure systems. The C_Z term is related to rising warm air and sinking cold air at the same latitude. The C_E term involves vertical transport of sensible heat, and is related to the horizontal variance of temperature. The C_A term is related to the transport of sensible heat across zonally averaged

meridional temperature gradients. The C_A and C_E terms are related to horizontal temperature gradients and are referred to as baroclinic terms. The C_K term corresponds to vertical and horizontal transport of momentum, and is referred to as the barotropic term. The analysis of the energy conversions associated with the formation and decay of a weather system separates the underlying atmospheric mechanisms into barotropic and baroclinic processes. The energy cascade from A_Z into K_E through A_E (indicated by the continuous blue line in Fig. 2), is referred to in the literature (Dias Pinto et al. 2013) as the baroclinic energy chain, since the involved conversion terms C_A and C_E are associated with baroclinic processes. The energy cascade from A_Z into K_E through K_Z (indicated by the dashed red line in Fig. 2), is on the other hand referred to as the barotropic chain, since it involves the C_K conversion term that is associated with barotropic processes.

Several studies applied the analysis of limited area energetics to study cyclones formation and intensification and the underlying processes (Michaelides 1987, 1992; Dias Pinto and Da Rocha 2011; Dias Pinto et al. 2013). Such studies showed in particular that the time series of the area-averaged vertical integrals of the energy conversion terms provide a way to assess the respective roles of barotropic and baroclinic processes in the cyclone intensification (Veiga et al. 2008; Pezza et al. 2014). This information provides further support to the analysis of storm structure (with cold core and warm core cyclones being respectively predominantly baroclinic and barotropic). On the other hand, the analysis of cyclone energetics is derived from large-scale environmental fields, and is thus less sensitive to the uncertainties affecting individual directly detected cyclone events.

Black and Pezza (2013) showed that cyclone energetics can be used as a proxy of explosive cyclogenesis, due to the robust and universal signatures found in the energy conversion terms. In this study, we adopt and extend their approach with the aim of identifying the processes playing a role in the rapid deepening of cyclones with different thermal structures. The information on the

cyclone energetics, and the associated barotropic and baroclinic mechanisms, is useful to better understand the cyclone intensification and its implications in terms of coastal impacts.

The energetics conversion terms are computed in the domain shown in Fig. 3. It has been shown (Pezza et al. 2014; Cavicchia et al. 2018) that a domain of such a size and shape is a good trade-off, since its extent allows the energetics features of storms influenced by both extra-tropical and tropical dynamics to be well captured, while at the same time it minimizes the chances that additional weather systems of a spatial scale comparable to the cyclone enter the domain at the same time.

f. Explosive cyclone development

One of the aims of the present work is to investigate the intensification pathways of ECLs, by focusing on the differences among the subset of cyclones that show a strong intensification and the larger set of cyclones in the region. Previous studies on ECLs have adopted different approaches to select the subset of very intense events, based on either the severity of impacts (Callaghan and Power 2014), or different metrics of intensity (Pepler et al. 2015).

Another commonly used metrics to identify cyclones that undergo a rapid intensification is the "bomb" criterion for explosive intensification introduced by Sanders and Gyakum (1980). The cyclone explosive deepening rate was defined by Sanders and Gyakum (1980) as a drop of the cyclone central pressure of more than 24 hPa over 24 hours relative to a latitude of 60 degrees:

$$\frac{\Delta p}{24}\frac{\sin 60}{|\sin\theta|} > 1 \tag{3}$$

An alternative definition, given by Lim and Simmonds (2002), is based on the deepening rate of relative pressure

$$\frac{\Delta p_a}{24}\frac{\sin 60}{|\sin\theta|} > 1 \tag{4}$$

where pressure anomalies p_a with respect to the climatology rather than absolute values are used, to avoid including spurious cases of cyclones that show an apparent deepening as they move across steep meridional pressure gradients, rather than deepening due to the cyclone central pressure drop itself. Allen et al. (2010) combined the two definitions into a combined explosive cyclone criterion, that identifies the cyclones that satisfy both conditions (3) and (4). The combined criterion was used by Black and Pezza (2013) to investigate the differences in the energetics properties of global climatologies of explosive cyclones with respect to ordinary cyclones.

Uncertainties in reanalyses for values of the storm central pressures are known to affect the number of low pressure systems identified as bomb cyclones. Allen et al. (2010) analyzed extensively the climatology of rapidly deepening cyclones in different reanalysis datasets. They found larger differences in the frequency of explosive cyclones in the southern hemisphere, due to sparser observations and larger storm track variability. Compared to other reanalysis products, it was found that ERA-Interim produce a larger number of rapidly deepening cyclones, due to its better representation of smaller systems.

A further possible source of ambiguity in the explosive cyclone definition lies in the different frequency at which atmospheric data are checked against the criterion, with some authors applying the criterion to every time step in the data (Black and Pezza 2013), while others only considering the 00 UTC time steps (Allen et al. 2010; Lim and Simmonds 2002). In this work, cyclone deepening is computed considering all ERA-Interim 6-hourly time steps, as we are comparing the results with the global analysis of Black and Pezza (2013).

3. Results

The analysis is based on the set of Australian ECLs identified in a 38-years period of ERA-Interim reanalysis data, from 1979 to 2016. The automated cyclone tracking and detection algo-

rithm described in Section 2c is applied. The total number of identified cyclones is 707, corresponding to an average frequency of occurrence of approximately 19 events per year. This figure is in good agreement with the reference value of 22 events per year given in Speer et al. (2009) over the same geographical area.

a. Cyclone classification

In order to systematically classify the detected cyclones, cyclone phase space parameters have been computed as described in Section 2.d for all the tracks. The values of the phase space parameters B, V_T^L and V_T^U are reported in Fig. 4 for every 6-hourly instance of all the detected cyclone tracks. Comparing Fig. 4 to Fig. 1, it is apparent that about two thirds of the cyclone tracks are composed of cold-cored cyclones, with the remaining third of the detected low pressures systems being hybrid cyclones, while a small but not negligible fraction of the set is characterized by a full warm core. Accordingly, the majority of cyclone instances are vertically tilted but approximately one third are vertically symmetric.

Given these relative fractions of the different dynamical structures, it is worthwhile to investigate whether the different cyclone classes are uniformly distributed in space, or whether some preferential geographical pattern emerges. To answer this question, the spatial distribution of the different cyclone classes is shown in Fig. 5. Here, every 6-hourly cyclone instance is depicted with a red dot if both $-V_T^L$ and $-V_T^U$ are positive, indicating a full warm core, with a blue dot if both $-V_T^L$ and $-V_T^U$ are negative, indicating a cold core, and with a yellow dot if $-V_T^L > 0$ and $-V_T^U < 0$, indicating a cyclone with hybrid features. It is evident from Fig. 5 that the different cyclone dynamical structures are not equally distributed in space. In the equatorward part of the region (north of approximately 22.5 $^\circ$ S), most of the cyclones instances are warm-cored cyclones, corresponding to tropical storms or tropical depressions entering the ECL domain from the north-

ern boundary. In the rest of the region, different cyclone structures coexist at the same latitudes, dominated by hybrid cyclone instances in the 22.5-32.5 ° S band, and by cold-cored cyclone instances south of 32.5 ° S. With respect to the warm core cyclones in the southern part of the domain, it is worth noticing that cyclone phase space alone does not distinguish tropical cyclones from warm seclusion extra-tropical cyclones (Hart 2003). The latitudinal gradient of occurrence of different types of cyclones is consistent with global climatologies of cyclone formation (Yanase et al. 2014). Important questions are, however, the quantification of the relative contribution of different classes of cyclone to the total ECL number as a function of latitude, and whether additional non-latitudinal occurrence spatial patterns are visible. The rest of this Section will focus on answering those questions.

Real-world cyclones, however, are not necessarily strictly bound to one of the three cyclone classes for all of their life cycle, since many cyclones transition between different classes once or even several times during their lifetime. While Fig. 5 gives information on the relative occurrence at different locations of the different cyclone phases, it is useful in order to quantify the relative occurrence of different types of low pressure systems to apply some criteria that assigns each cyclone to a single class. Here we adopt the simplest possible criterion i.e. we count the number of time steps a cyclone is classified in each of the dynamical phases and we assign it to the prevailing class, the one that corresponds to the majority of the time steps during the cyclone lifetime. The number of cyclones classified in each class is reported in the first line of Table 1. The classification is performed using all time steps in the tracked cyclone lifetime. In order to take into account the sensitivity of the cyclone properties on the details of the classification, some of the results are also shown (supplementary Figures S2 and S3) for a modified version of the classification definition, where only time steps where the cyclone is inside the domain shown in Fig. 3 are used. Figure 6 shows for each class the fraction of cyclone duration the cyclone stays in the same class. Overall,

warm core cyclones transition between classes for 40% of their duration on average, compared to 35% for hybrid cyclones and just 20% for cold core cyclones. While the warm core cyclone tracks forming north of 25 ° S seem to be associated with (transitioning) tropical cyclones, the warm core tracks with a genesis location closer to the pole are interpreted as warm seclusion cyclones. It has previously been shown that the Tasman Sea is a global hotspot for warm seclusion extra-tropical cyclone occurrence (Maue 2010). In the following, only proper warm core cyclones are considered in the analysis. In order to exclude warm seclusion events, warm core cyclones with an average latitude southward of 35 ° S are discarded (supplementary Fig. S1). Note that only the tropical lows that form north of the analysis domain shown in Fig. 3 and have a detected instance within this domain are counted or included in the analysis. This would exclude the majority of tropical cyclones that form off eastern Australia and do not move south of 24 ° S. The global seasonality of warm-core and cold-core cyclones is relatively well understood and reproduced in our results. The seasonality of hybrid cyclones, on the other hand, exhibits a larger variability, depending on the region where they occur (da Rocha et al. 2018), due to the influence of circulation patterns on the associated upper level cut-off/troughs.

ECLs are observed year-round, but the peak in their frequency as well as the most intense and damaging events tend to occur in the transition to the cold season (Holland et al. 1987). Here we investigate if cyclones with different dynamical features have differing seasonality. Figure 7 shows the relative contribution of the three classes of respectively cold-core, hybrid and warm-core cyclones to the total seasonal cycle according to the cyclone's average latitude. As Fig. 7 shows, the overall seasonal cycle is dominated by cold core cyclones, which have a higher frequency in the Southern Hemisphere cold season. The warm core cyclones on the other hand tend to occur in the warm season, while the frequency of hybrid cyclones is more uniform throughout the year. The majority of cyclones with a mean cyclone track latitude south of 32.5 ° S are cold core cyclones

with a prevailing winter occurrence. A non-negligible fraction of the low pressure systems in this area are hybrid systems, however. The majority of cyclones with a mean cyclone track latitude between 22.5 ° S and 32.5 ° S are hybrid cyclones with enhanced activity in the warm season. Finally, the few tracks with a mean cyclone track latitude north of 22.5 ° S are mostly warm core cyclones.

Fig. 8 shows the interannual time series for the three classes of cyclones. It is worth noticing that the interannual variability is large for all kind of cyclones, but it is larger for warm core than for hybrid and cold core cyclones (coefficients of variation respectively 0.28 for cold core, 0.72 for hybrid and 1.82 for warm core cyclones). On the other hand, the correlation among the different classes is rather weak (correlation coefficients respectively 0.16 for warm core and cold core, 0.13 for cold core and hybrid, and 0.01 for hybrid and warm core). No statistically significant trends emerge in the time series. The correlation with ENSO (NINO3.4 index) has been checked for the different cyclone classes and geographical regions, and found to be generally weak (not shown).

So far we have discussed the general properties, from formation to dissipation, of all cyclones that enter for some time into the ECL region (shown in Fig 3). In the rest of the present subsection, we are focusing on the interior of the ECL region, discussing in more detail the properties of the cyclones once they enter and stay in the region. A clear meridional stratification is evident in the average latitude, within the area, of the three classes of cyclones, with the average latitude of warm core cyclones closer to the equator-ward boundary of the region (at approximately 30 ° S), the average latitude of hybrid cyclones almost five degrees further south (at approximately 35 ° S), and the average latitude of cold core cyclones further displaced polewards (at approximately 37 ° S). Figure 9 shows the the zonal and meridional stratification of the different classes of low pressure systems. The top panel of Fig. 9 shows the relative fraction of each class of cyclones with respect to the total cyclone number, averaged as a function of latitude. There is a clear link

between the increase of the fraction of hybrid cyclones and the decrease of cold core cyclone fraction, moving equatorwards from the southern boundary of the domain. The fractions of the two classes of cyclones show comparable values at approximately 32 ° S. The fraction of warm core cyclones becomes substantially larger than 0 only north of 30 ° S. The bottom panel of Fig. 9 shows the relative fraction of each class of cyclones with respect to the total cyclone number, averaged as a function of the distance from the coast. It is found that hybrid cyclones have an enhanced activity closer to the coast than further offshore. Within approximately 5 degrees from the coast, the fraction of hybrid cyclones exceeds 30 %, reaching 45 % between 2 and 3 degrees from the coast, and then gradually decreases moving further away from the coast. The warm core cyclone fraction also decreases moving away from the coast. Cold core cyclones on the other hand are more than two thirds of the total further than 5 degrees from the coast, while they decrease to less than two thirds closer to the coast. If cyclones are classified using only time steps within the ECL domain both the zonal and meridional stratification of hybrid and cold core cyclones are more marked (supplementary Fig. S3) supporting the main conclusion that hybrid cyclones have a stronger activity closer to the tropics and closer to the coast. The enhanced coastal activity of hybrid cyclones is an interesting finding, given its potential implications for extreme weather hazards on the coastline.

Figure 10 shows the normalized distribution of two different pressure-based intensity metrics for the three classes of cyclones, with these two metrics being the lowest value of mean sea level pressure anomalies (with respect to the climatological monthly values at a given location) and the largest value of mean sea level pressure Laplacian registered along the cyclone track. Even though the tail of sea level pressure Laplacian distribution shows more events for hybrid than for cold core cyclones, the difference between distributions is not significant at the 95 % level.

b. Cyclone intensification and energetics

One of the goals of this work is to investigate whether the intensification of different classes of cyclones is driven by different processes in the atmosphere. In order to do so, we study the energetics of the subset of rapidly intensifying cyclones for the three classes of warm core hybrid and cold core cyclones. Previous studies Black and Pezza (2013) have shown that robust signatures are found in the energetics of explosively intensifying extra-tropical cyclones, characterized by statistically significant peaks in the baroclinic conversion terms at the time of cyclone maximum deepening, while the barotropic term showed only fluctuations around zero. Given the significant fraction of hybrid cyclones among ECLs, the question we aim to answer is whether their energetics is characterized by different signatures with respect to the cold core cyclones.

The second question we aim to address is whether there are significant differences in the energetics of rapidly intensifying and non-rapidly intensifying cyclones, both in terms of the dominant processes involved and of the strength of the energy conversions. This is a relevant question not only because it can shed some light on the physical processes underlying cyclone intensification, but also it can indicate whether the diagnostics based on the cyclone energetics can potentially be used as a proxy to estimate cyclone intensities. In order to answer this question we divide cyclones into three subset of according to their deepening rate: explosive cyclones, cyclones with a rate of deepening half that one of explosive cyclones ("half bomb" cyclones) and non -rapidly intensifying cyclones (with a rate of deepening less than half that of explosive cyclones).

The analysis is performed following the approach of Black and Pezza (2013). In this approach, the first step is to identify bomb cyclones applying the criterions described in Section 2.f. Both the original definition (Sanders and Gyakum 1980) of explosive deepening and the combined criterion of Allen et al. (2010) have been used. Composites of the time series of anomalies of energetics

conversion terms are then created. In order to create the composite, a reference time for the different cyclones in the composite is needed: this is achieved by defining for each storm as the time $t = 0$ the first time step in the cyclone lifetime that is followed by a 24 hours explosive deepening phase. The energetics composites are calculated for the three classes of hybrid cold-core and warm-core cyclones separately. In order to compare the energetics of rapidly intensifying and non rapidly intensifying cyclones, the composites are also calculated for cyclones whose deepening rate is below the threshold defined in Eqn. 3 but above half the threshold value, and for cyclones with a deepening rate less than half the threshold value.

The number of cyclones identified in each intensity set and dynamical class, for the two variations of the explosive deepening rate criterion, are summarized in Table 1. The number of detected explosively deepening cyclones sum up to 17% and 9% (according to respectively the original and combined explosive deepening rate definitions) of the number of cyclones with a duration of 24 hours of more.

The results of the energetics analysis are shown in Fig. 11 for the original deepening criterion. The corresponding analysis using the combined explosive deepening criterion is shown in supplementary Fig. S4. The differences between the two approaches are small, also noting that the low sensitivity of the analysis on the chosen criterion adds to the robustness of the results. Given the small sample size of warm core cyclones the composite of warm core cyclones is shown only for explosively deepening cyclones. The first notable result is that the barotropic term C_K shows a non-negligible signature for all subsets of cyclones, in contrast to the global case of Black and Pezza (2013) where the same term was found to show only fluctuations around zero. This difference can be explained by the fact that in the analysis of Black and Pezza (2013) the hemispheric composite is dominated by mid-latitude events, developing in a region of the atmosphere characterized by a high baroclinicity; the analysis in the current work, on the other hand, is focused on a smaller

region in the subtropics, where the barotropic processes have an enhanced role in the atmosphere. The barotropic term is dominant for warm core cyclones, while for hybrid cyclones the barotropic and baroclinic terms have comparable amplitudes. For the cold core cyclones, baroclinic terms are dominant but the barotropic term is non-negligible. The finding that the intensification of cold core cyclones can also be partly driven by barotropic processes is consistent with Fig. 6 showing that cold core cyclones have on average a transition to a hybrid phase for a significant portion of their lifetime. One example of the transition of a mostly cold core cyclone to a hybrid structure at the peak of intensification was illustrated in Cavicchia et al. (2018) analyzing the well known case of the Pasha Bulker cyclone. The signature in the baroclinic terms is similar to the one found in the global case, with a peak in the C_A and C_E terms corresponding to the period of explosive deepening for both hybrid and cold core cyclones, but that the peak of the baroclinic C_E term has a larger amplitude for the hybrid cyclones than for the cold core cyclones. Another interesting difference is that, while for the hybrid cyclones the peaks of the barotropic and baroclinic terms are in phase, for the cold core cyclones the peak of the barotropic C_K term precedes the peak of the baroclinic C_E and C_A terms, with a lag of approximately 24 hours. This might give an indication that barotropic energy conversion processes precondition the atmosphere for subsequent more efficient baroclinic conversion, by transferring kinetic energy from the zonal mean flow to the disturbance (Dias Pinto et al. 2013). This behavior of the energy conversion terms could indicate a development similar to the type B cyclogenesis of Petterssen and Smebye (1971), where the first phase of an extra-tropical cyclone formation is characterized by a transient barotropic growth as a cyclogenesis precursor, associated with the passage of an upper-level feature over a baroclinic region (Kucharski and Thorpe 2001; Plant et al. 2003). The half bomb cyclones and non-rapidly intensifying cyclones subsets show similar signatures with respect to the bomb cyclones subset, but the peaks of the different energy conversion terms show reduced amplitude. This gives an

indication that for non-rapidly intensifying cyclones the energy exchanges are less vigorous, but the physical processes involved in the intensification of cyclones with the same thermal structure but different rates of deepening do not vary substantially.

4. Discussion and Conclusions

a. Summary and Discussion

The purpose of the present work is to systematically explore new directions in the understanding of the multi-decadal climatology of the occurrence and intensification of Australian east coast cyclones. The goal is pursued by classifying ECLs according to their thermal structure as respectively warm core, hybrid and warm core cyclones. The environment energetics at the time of cyclone occurrence is then analyzed for rapidly intensifying and non-rapidly intensifying cyclones of different classes, in order to investigate the different role of barotropic and baroclinic processes in cyclone intensification.

Previous classifications of ECLs into different subtypes exist. Notable examples are the ones of Holland et al. (1987) and Browning and Goodwin (2013). The present classification of ECLs based on thermal structure is not intended as a replacement of those previous classification, but rather to complement them addressing some aspects that have been identified as knowledge gaps. Holland et al. (1987) identified three subtypes of ECLs, based on the location of the storm with respect to synoptic systems known as easterly dips. Browning and Goodwin (2013) classified ECLs into five categories based on cyclone location and propagation direction, following the definitions used in Public Works Department (PWD) (1985). Both the aforementioned studies identified the concurrent influence of baroclinic and diabatic forcing on the storms, and acknowledged to some extent the hybrid/warm core nature of the low pressure systems in the mature stage of the cyclone

lifetime. The difference of our approach lies in that, since the main aim of the present work is the quantification of the occurrence of cyclones with different structures, we use the information on the cyclone thermal structure as a primary classification criterion rather than an *a posteriori* diagnostic. Also, in the present study the cyclone phase space analysis is applied systematically for all the time steps of all the detected events, rather than for selected subset of events. This approach is useful and needed, on the one hand, to improve the understanding of ECL formation in the context of global subtropical/hybrid cyclones occurrence. On the other hand, such classification is potentially useful for the analysis of ECLs coastal impacts and damage, since different ECL dynamical types are expected to be associated to different impacts. The last aspect, however, is not a focus of the present work.

We find that about one third of the detected cyclones are low pressure systems with a prevailing hybrid structure. A smaller set of events consist of warm core cyclones that are ex-tropical cyclones entering the ECL region from the northern boundary. The remaining two thirds of cyclones have a cold core structure for the largest part of their lifetime; however, most of the cold core cyclones transition to the hybrid phase for a significant portion (20 % on average) of their lifetime. Many storms enter the ECL region after they have formed elsewhere. If only the time-steps within the ECL region are used for the classification, the fraction of hybrid cyclones increases. This finding agrees with previous results of Holland et al. (1987) and Browning and Goodwin (2013) on the common occurrence of hybrid cyclones among ECLs. Previous studies did not quantify the relative occurrence of cyclones with different thermal structure; the current work fills this knowledge gap. We also find that the occurrence of hybrid cyclones is enhanced in the northern part of the ECL region and closer to the coast. These results also add to the existing knowledge on this topic, as previous studies did not investigate in depth the spatial patterns within the ECL region of cyclones with different thermal structure. Furthermore, we find that the activity of cold core cy-

clones is larger in winter, while the seasonality of hybrid cyclones is less marked. While based on a different approach providing additional and more systematical information on the storm thermal structure and being based on physical variables only rather than making additional assumption on the cyclone location or motion, our results are broadly consistent with the findings of Browning and Goodwin (2013). They analyzed the cyclone phase space for two of the subtypes of events considered in the study: the ETL (easterly trough lows) events that track in a southern direction and the SSL (southern secondary lows) events that move over the ocean in a northerly direction. They found that on average ETL events have initially a baroclinic structure while transitioning to a hybrid structure after the second day and to a warm core structure after the fouth day, while SSL events develop a hybrid structure by the third day but do not transition to a warm core. They also find that SSL events are more common in winter while ETL events are more common year-round. It thus appears likely that there is a large overlap among the cyclones classified as cold core and the SSL events on the one hand, and among hybrid cyclones and ETL events on the other hand. This study, however, extends the analysis of cyclone phase space to the full set of cyclones occurring in the ECL region.

Concerning the analysis of the storms energetics, the current work builds up on the analysis of Black and Pezza (2013) that found a global and universal signature in the energetics of the explosively deepening cyclones. They found that the time series of the baroclinic energy conversion terms is characterized by a peak corresponding to the phase of rapid intensification, while the barotropic conversion terms only shows non statistically significant fluctuations. Here, we contrast their results, that were based mostly on extra-tropical storms, showing that in the case of rapidly deepening ECLs the barotropic conversion terms play a significant role for all classes of cyclones. Barotropic energy conversions are dominant for warm core cyclones, while for hybrid cyclones the barotropic and baroclinic energy conversions have comparable strengths. Even for the cold

core cyclones, the barotropic terms are non negligible. This result is consistent with the cyclone thermal classification, as we find that most cold core cyclones have a transition to an hybrid phase for a significant amount of time. The significance of the results lies on the one hand on the fact that the cyclone structure has been linked to the different physical mechanisms underlying cyclone formation and intensification. On the other hand, it has been shown that the intensification pathways of explosively deepening cyclones in the subtropics significantly differ from their mid-latitude counterpart, being characterized by a different balance of the barotropic and baroclinic terms.

Investigating in depth the environmental factors driving the evolution of the cyclone thermal structure and intensification is beyond the scope of the present work. However, we took an intermediate step, and analyzed the surface heat fluxes associated with the three different classes of cyclones. The presence of large latent and sensible heat fluxes associated to a cyclone indicates the role of surface forcing and barotropic processes and is expected to lead to positive thermal anomalies close to the surface. Figure 12 shows the composites for the three classes of cyclones of the time series of along-the-track sensible and latent heat fluxes, averaged within a 4 degrees lat-lon box centered on the cyclone sea surface pressure minimum. The composite is calculated by setting as the origin of the time axis the time step corresponding to the lifetime lowest sea level pressure minimum. As Fig. 12 shows, the largest values of both latent and sensible heat fluxes are found for warm core cyclones, decreasing for hybrid cyclones while cold core cyclones show the smallest values. Interestingly, the difference between the three classes of cyclones are large in the intensification phase (the 48-hours period preceding the maximum intensity), but are largely reduced after the cyclone has reached its lifetime minimum pressure. The analysis of surface fluxes, shows that, consistent with the previous understanding of different types of cyclones, air-sea interactions are relevant for warm-core cyclones, while they are much less so for the cold-core ones. The analysis also show that air-sea interaction also plays a role in the intensification phase of hy-

brid cyclones, even if such role is not dominant as in the case of warm core cyclones due to the presence of additional processes.

b. Conclusions and Outlook

In this study, results from a physically motivated climatology of Australian ECLs occurrence and intensification have been presented and discussed, based on a classification of low pressure systems according to their dynamical structure and on the analysis of the environment energetics in the cyclone surroundings.

While addressing some existing knowledge gaps, this work on the other hand paves the way for further investigation on a number of aspects concerning present and future ECL activity at a number of timescales, and the associated impacts.

A direction of further investigation is to assess how the impacts of different classes of ECLs such as hybrid or cold core cyclones differ, in terms of wind, rainfall or other variables along the lines of a similar analysis of Kiem et al. (2016) for cyclones with a different origin.

The results of the present work provide a framework to address a number of open questions related to the properties of ECLs in future climate projections. One aspect is whether climate change will affect different classes of low pressure systems in similar or different ways, e.g. by altering the relative fraction or the spatial patterns of warm core, hybrid and cold core systems. Such alteration can cause changes in the associated impacts if the impacts of different classes of cyclones differ substantially (Kiem et al. 2016). Furthermore, there are several indications of a poleward migration of tropical cyclone activity following the expansion of the tropics in a warmer climate (Walsh and Katzfey 2000; Lavender and Walsh 2011; Kossin et al. 2014; Parker et al. 2018; Studholme and Gulev 2018; Sharmila and Walsh 2018). It would therefore be of great interest to complement those findings by analysing the projected changes in the meridional stratification of the cyclone

spectrum in a set of climate model projections. Studies on global atmospheric energetics (Veiga and Ambrizzi 2013) showed that in a warming world both the baroclinic energy conversion term C_A and the barotropic conversion term C_K are significantly altered. The term C_A decreases, as a consequence of the reduction of sensible heat transport by eddies due to decreased horizontal temperature gradients. Barotropic processes creating eddy transport of angular momentum on the other hand increase, contributing to the increase of the term C_K. The effect of such changes of the energy cycle on the intensification of cyclones has not been investigated in the literature so far.

A further direction worth investigating is the potential impact of the findings of the present work on the predictability of cyclone impacts. The rapid intensification of cyclones is notably difficult to forecast, due to the lack of understanding of the detail of mechanisms driving it. The energetics analysis could thus serve as a guidance for forecast assessments introducing additional diagnostics for cyclone intensification, complementing the information obtained from high-resolution numerical weather prediction models. In addition, the predictability of cyclones on longer timescales might be better explained if the contributions from different cyclone classes are considered.

Finally, the results shown have potential implications for cyclone climatologies in other regions, where tropical-extratropical interactions play a role in cyclone formation and intensification. The systematic application of similar analysis to other subtropical basins, and possibly at the global scale, is worthy of further investigation to improve the understanding of the response of the cyclone spectrum in its complexity to variations in the state of climate.

Acknowledgments. This research was supported through funding from the Earth System and Climate Change Hub of the Australian Government's National Environmental Science Programme.

References

Allen, J. T., A. B. Pezza, and M. T. Black, 2010: Explosive cyclogenesis: A global climatology comparing multiple reanalyses. *J. Climate*, **23**, 6468–6484.

Black, M. T., and A. B. Pezza, 2013: A universal, broad-environment energy conversion signature of explosive cyclones. *Geophys. Res. Lett.*, **40**, 452–457.

Browning, S. A., and I. D. Goodwin, 2013: Large-scale influences on the evolution of winter subtropical maritime cyclones affecting Australia's east coast. *Mon. Wea. Rev.*, **141**, 2416–2431.

Callaghan, J., and S. B. Power, 2014: Major coastal flooding in southeastern Australia 1860–2012, associated deaths and weather systems. *Aust. Meteor. Ocean. J.*, **64**, 183–213.

Caruso, S. J., and S. Businger, 2006: Subtropical cyclogenesis over the central North Pacific. *Wea. Forecasting*, **21**, 193–205.

Cavicchia, L., A. Dowdy, and K. Walsh, 2018: Energetics and Dynamics of Subtropical Australian East Coast Cyclones: Two Contrasting Cases. *Mon. Wea. Rev.*, **146**, 1511–1525.

Cavicchia, L., H. von Storch, and S. Gualdi, 2014: A long-term climatology of medicanes. *Climate Dyn.*, **43**, 1183–1195.

Clarke, R., 1956: A study of cyclogensis in relation to the contours of the 300mb surface. *Aust. Meteor. Mag.*, **12**, 1–21, [Available online at http://www.bom.gov.au/jshess/docs/1956/clarke.pdf].

da Rocha, R. P., M. S. Reboita, L. F. Gozzo, L. M. M. Dutra, and E. M. de Jesus, 2018: Subtropical cyclones over the oceanic basins: A review. *Ann. N.Y. Acad. Sci.*, **1436**, 138–156.

Dee, D. P., and Coauthors, 2011: The ERA-Interim reanalysis: Configuration and performance of the data assimilation system. *Quart. J. Roy. Meteor. Soc.*, **137**, 553–597.

Di Luca, A., J. P. Evans, A. Pepler, L. Alexander, and D. Argüeso, 2015: Resolution sensitivity of cyclone climatology over eastern Australia using six reanalysis products. *J. Climate*, **28**, 9530–9549.

Dias Pinto, J. R., and R. P. Da Rocha, 2011: The energy cycle and structural evolution of cyclones over southeastern South America in three case studies. *J. Geophys. Res.: Atmos.*, **116**, D14 112.

Dias Pinto, J. R., M. S. Reboita, and R. P. Rocha, 2013: Synoptic and dynamical analysis of subtropical cyclone Anita (2010) and its potential for tropical transition over the South Atlantic Ocean. *J. Geophys. Res.: Atmos.*, **118**, 10 870–10 883.

Dowdy, A. J., G. A. Mills, and B. Timbal, 2013: Large-scale diagnostics of extratropical cyclogenesis in eastern Australia. *Int. J. Climatol.*, **33**, 2318–2327.

Evans, J. L., and A. Braun, 2012: A climatology of subtropical cyclones in the South Atlantic. *J. Climate*, **25**, 7328–7340.

Garde, L. A., A. B. Pezza, and J. A. T. Bye, 2010: Tropical transition of the 2001 Australian Duck. *Mon. Wea. Rev.*, **138**, 2038–2057.

González-Alemán, J. J., F. Valero, F. Martín-León, and J. L. Evans, 2015: Classification and synoptic analysis of subtropical cyclones within the northeastern Atlantic Ocean. *J. Climate*, **28**, 3331–3352.

Gozzo, L. F., R. P. da Rocha, M. S. Reboita, and S. Sugahara, 2014: Subtropical cyclones over the southwestern South Atlantic: Climatological aspects and case study. *J. Climate*, **27**, 8543–8562.

738 Guishard, M. P., J. L. Evans, and R. E. Hart, 2009: Atlantic subtropical storms. Part II: climatol-
739 ogy. *J. Climate*, **22**, 3574–3594.

740 Hart, R. E., 2003: A cyclone phase space derived from thermal wind and thermal asymmetry.
741 *Mon. Wea. Rev.*, **131**, 585–616.

742 Hewson, T. D., and U. Neu, 2015: Cyclones, windstorms and the IMILAST project. *Tellus*, **67**,
743 27 128.

744 Hodges, K., A. Cobb, and P. L. Vidale, 2017: How well are tropical cyclones represented in
745 reanalysis datasets? *J. Climate*, **30**, 5243–5264.

746 Hodges, K. I., R. W. Lee, and L. Bengtsson, 2011: A comparison of extratropical cyclones in
747 recent reanalyses: ERA-Interim, NASA MERRA, NCEP CFSR, and JRA-25. *J. Climate*, **24**,
748 4888–4906.

749 Holland, G. J., A. H. Lynch, and L. M. Leslie, 1987: Australian east-coast cyclones. Part I: Syn-
750 optic overview and case study. *Mon. Wea. Rev.*, **115**, 3024–3036.

751 Hopkins, L. C., and G. J. Holland, 1997: Australian heavy-rain days and associated east coast
752 cyclones: 1958–92. *J. Climate*, **10**, 621–635.

753 Johnson, D. R., 1970: The available potential energy of storms. *J. Atmos. Sci.*, **27**, 727–741.

754 Kiem, A. S., C. Twomey, N. Lockart, G. Willgoose, G. Kuczera, A. K. Chowdhury, N. P. Manage,
755 and L. Zhang, 2016: Links between East Coast Lows and the spatial and temporal variability
756 of rainfall along the eastern seaboard of Australia. *J. South. Hemisphere Earth. Syst. Sci.*, **66**,
757 162–176.

758 Kossin, J. P., K. A. Emanuel, and G. A. Vecchi, 2014: The poleward migration of the location of
759 tropical cyclone maximum intensity. *Nature*, **509**, 349.

760 Kraus, E., 1954: Secular changes in the rainfall regime of SE. Australia. *Quart. J. Roy. Meteor.*
761 *Soc.*, **80**, 591–601.

762 Kucharski, F., and A. J. Thorpe, 2001: The influence of transient upper-level barotropic growth on
763 the development of baroclinic waves. *Quart. J. Roy. Meteor. Soc.*, **127**, 835–844.

764 Lavender, S., and K. Walsh, 2011: Dynamically downscaled simulations of Australian region
765 tropical cyclones in current and future climates. *Geophys. Res. Lett.*, **38**.

766 Lim, E.-P., and I. Simmonds, 2002: Explosive cyclone development in the Southern Hemisphere
767 and a comparison with Northern Hemisphere events. *Mon. Wea. Rev.*, **130**, 2188–2209.

768 Lorenz, E. N., 1955: Available potential energy and the maintenance of the general circulation.
769 *Tellus*, **7**, 157–167.

770 Maue, R. N., 2010: Warm seclusion extratropical cyclones. Ph.D. thesis, The Florida State Uni-
771 versity.

772 Mauk, R. G., and J. S. Hobgood, 2012: Tropical cyclone formation in environments with cool SST
773 and high wind shear over the northeastern Atlantic Ocean. *Wea. Forecasting*, **27**, 1433–1448.

774 Michaelides, S. C., 1987: Limited area energetics of Genoa cyclogenesis. *Mon. Wea. Rev.*, **115**,
775 13–26.

776 Michaelides, S. C., 1992: A Spatial and Temporal Energetics Analysis of a Baroclinic Disturbance
777 in the Mediterranen. *Mon. Wea. Rev.*, **120**, 1224–1243.

778 Miglietta, M., S. Laviola, A. Malvaldi, D. Conte, V. Levizzani, and C. Price, 2013: Analysis of
779 tropical-like cyclones over the Mediterranean Sea through a combined modeling and satellite
780 approach. *Geophys. Res. Lett.*, **40**, 2400–2405.

781 Mills, G. A., R. Webb, N. E. Davidson, J. Kepert, A. Seed, and D. Abbs, 2010: The Pasha Bulker
782 east coast low of 8 June 2007. Centre for Australian Weather and Climate Research Tech. Rep.,
783 62 pp. [Available online at www.cawcr.gov.au/technical-reports/CTR_023.pdf].

784 Murray, R. J., and I. Simmonds, 1991: A numerical scheme for tracking cyclone centres from
785 digital data. *Aust. Meteorol. Mag.*, **39**, 155–166.

786 Neu, U., and Coauthors, 2013: IMILAST: A community effort to intercompare extratropical cy-
787 clone detection and tracking algorithms. *Bull. Amer. Meteor. Soc.*, **94**, 529–547.

788 Otkin, J. A., and J. E. Martin, 2004: A synoptic climatology of the subtropical kona storm. *Mon.*
789 *Wea. Rev.*, **132**, 1502–1517.

790 Parker, C. L., C. L. Bruyère, P. A. Mooney, and A. H. Lynch, 2018: The response of land-falling
791 tropical cyclone characteristics to projected climate change in northeast Australia. *Climate Dyn.*,
792 1–19.

793 Pepler, A., and A. Coutts-Smith, 2013: A new, objective, database of East Coast Lows. *Aust.*
794 *Meteorol. Ocean. J.*, **63**, 461–472.

795 Pepler, A. S., A. Di Luca, and J. P. Evans, 2017: Independently assessing the representation of
796 midlatitude cyclones in high-resolution reanalyses using satellite observed winds. *Int. J. Clima-*
797 *tol.*, doi:10.1002/joc.5245.

798 Pepler, A. S., A. Di Luca, F. Ji, L. V. Alexander, J. P. Evans, and S. C. Sherwood, 2015: Impact
799 of identification method on the inferred characteristics and variability of Australian East Coast
800 Lows. *Mon. Wea. Rev.*, **143**, 864–877.

801 Petterssen, S., and S. J. Smebye, 1971: On the development of extratropical cyclones. *Quart. J.*
802 *Roy. Meteor. Soc.*, **97**, 457–482.

Pezza, A. B., L. A. Garde, J. A. P. Veiga, and I. Simmonds, 2014: Large scale features and energetics of the hybrid subtropical low Duck over the Tasman Sea. *Climate Dyn.*, **42**, 453–466.

Pinto, J. G., T. Spangehl, U. Ulbrich, and P. Speth, 2005: Sensitivities of a cyclone detection and tracking algorithm: individual tracks and climatology. *Meteor. Z.*, **14**, 823–838.

Plant, R., G. C. Craig, and S. Gray, 2003: On a threefold classification of extratropical cyclogenesis. *Quart. J. Roy. Meteor. Soc.*, **129**, 2989–3012.

Public Works Department (PWD), 1985: Elevated coastal levels; Storms affecting N.S.W. coast 1880-1980. Weatherex Meteorological Services and Public Works Department Rep. 85041, 574 pp.

Raible, C., P. Della-Marta, C. Schwierz, H. Wernli, and R. Blender, 2008: Northern Hemisphere extratropical cyclones: A comparison of detection and tracking methods and different reanalyses. *Mon. Wea. Rev.*, **136**, 880–897.

Sanders, F., and J. R. Gyakum, 1980: Synoptic-dynamic climatology of the bomb. *Mon. Wea. Rev.*, **108**, 1589–1606.

Sharmila, S., and K. Walsh, 2018: Recent poleward shift of tropical cyclone formation linked to Hadley cell expansion. *Nature Climate Change*, doi:10.1038/s41558-018-0227-5.

Simmonds, I., C. Burke, and K. Keay, 2008: Arctic climate change as manifest in cyclone behavior. *J. Climate*, **21**, 5777–5796.

Simmonds, I., R. J. Murray, and R. M. Leighton, 1999: A refinement of cyclone tracking methods with data from FROST. *Aust. Meteor. Mag.*, Special Edition, 35–49, [Available online at http://www.bom.gov.au/jshess/docs/1999/simmonds.pdf].

824 Smith, P. J., 1969: On the contribution of a limited region to the global energy budget. *Tellus*, **21**,
825 202–207.

826 Speer, M. S., P. Wiles, A. Pepler, and Coauthors, 2009: Low pressure systems off the New South
827 Wales coast and associated hazardous weather: establishment of a database. *Aust. Meteorol.*
828 *Ocean. J.*, **58**, 29–39.

829 Studholme, J., and S. Gulev, 2018: Concurrent Changes to Hadley Circulation and the Meridional
830 Distribution of Tropical Cyclones. *J. Climate*, **31**, 4367–4389.

831 Veiga, J. A. P., and T. Ambrizzi, 2013: A global and hemispherical analysis of the Lorenz ener-
832 getics based on the representative concentration pathways used in CMIP5. *Adv. Meteor.*, **2013**,
833 1–13.

834 Veiga, J. A. P., A. B. Pezza, I. Simmonds, and P. L. Silva Dias, 2008: An analysis of the environ-
835 mental energetics associated with the transition of the first South Atlantic hurricane. *Geophys.*
836 *Res. Lett.*, **35**, L15 806.

837 Walsh, K., F. Giorgi, and E. Coppola, 2014: Mediterranean warm-core cyclones in a warmer
838 world. *Climate Dyn.*, **42**, 1053–1066.

839 Walsh, K. J., and J. J. Katzfey, 2000: The impact of climate change on the poleward movement of
840 tropical cyclone–like vortices in a regional climate model. *J. Climate*, **13**, 1116–1132.

841 Yanase, W., H. Niino, K. Hodges, and N. Kitabatake, 2014: Parameter spaces of environmental
842 fields responsible for cyclone development from tropics to extratropics. *J. Climate*, **27**, 652–671.

843 Zappa, G., L. Shaffrey, and K. Hodges, 2014: Can polar lows be objectively identified and tracked
844 in the ECMWF operational analysis and the ERA-Interim reanalysis? *Mon. Wea. Rev.*, **142**,
845 2596–2608.

LIST OF TABLES

TABLE 1. Number of cold core (CC), hybrid (HC) and warm core (WC) tracks (warm seclusion type events are removed form the counting). First to last row: total climatology; the set of bomb cyclones identified with the original explosive deepening criterion; the set of half bomb cyclones identified with the original explosive deepening criterion; the set of bomb cyclones identified with the combined explosive deepening criterion; the set of half bomb cyclones identified with the combined explosive deepening criterion.

	TOT	*CC*	%	*HC*	%	*WC*	%
Total climatology	707	532	78%	140	20%	7	2%
Bomb cyclones (original)	122	91	75%	25	20%	3	3%
Half bomb cyclones (original)	327	256	78%	67	20%	2	1%
Bomb cyclones (combined)	64	41	64%	17	26%	3	5%
Half bomb cyclones (combined)	285	217	76%	64	22%	2	1%

LIST OF FIGURES

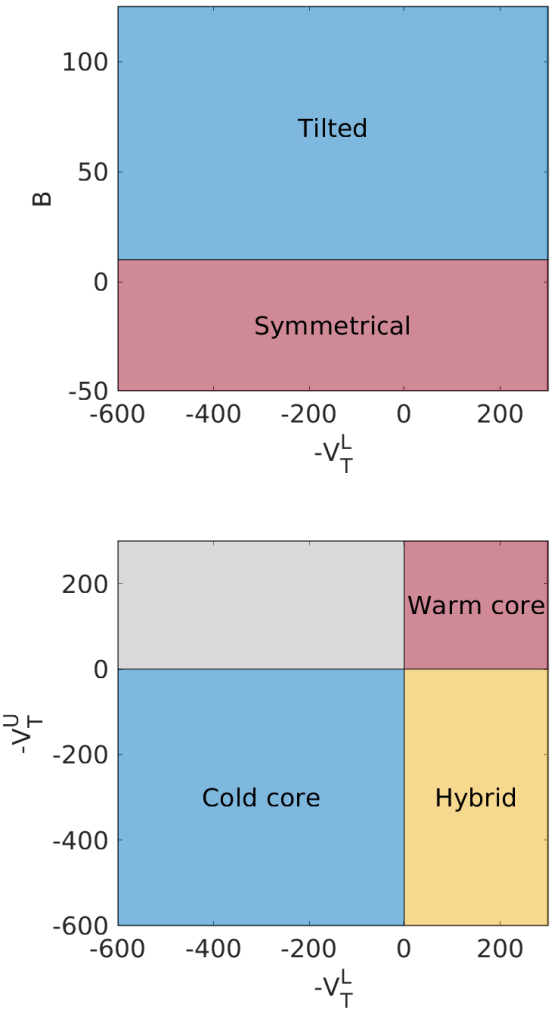

912 FIG. 1. Schematic representation of the cyclone phase space diagrams. Top: lower troposphere warm core
913 (x axis) and symmetry parameter (y axis): the red shaded area indicates vertically symmetric cyclones, the blue
914 shaded area indicates vertically tilted cyclones. Bottom: lower troposphere thermal core (x axis) and upper
915 troposphere thermal core (y axis): the red shaded area indicates fully warm-core cyclones, the blue shaded area
916 indicates fully cold-core cyclones, and the yellow shaded area indicates hybrid cyclones.

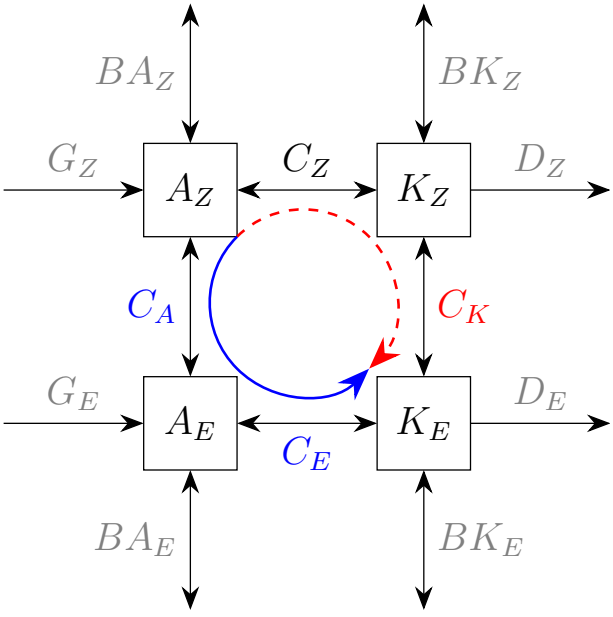

FIG. 2. Schematic representation of the different terms in the energy cycle as described in the manuscript. The terms in the squared boxes are the energy terms. The terms in gray are generation, dissipation and boundary terms. The C terms are the energy conversion terms. Blue labels and lines indicate baroclinic processes, red labels and lines indicate barotropic processes.

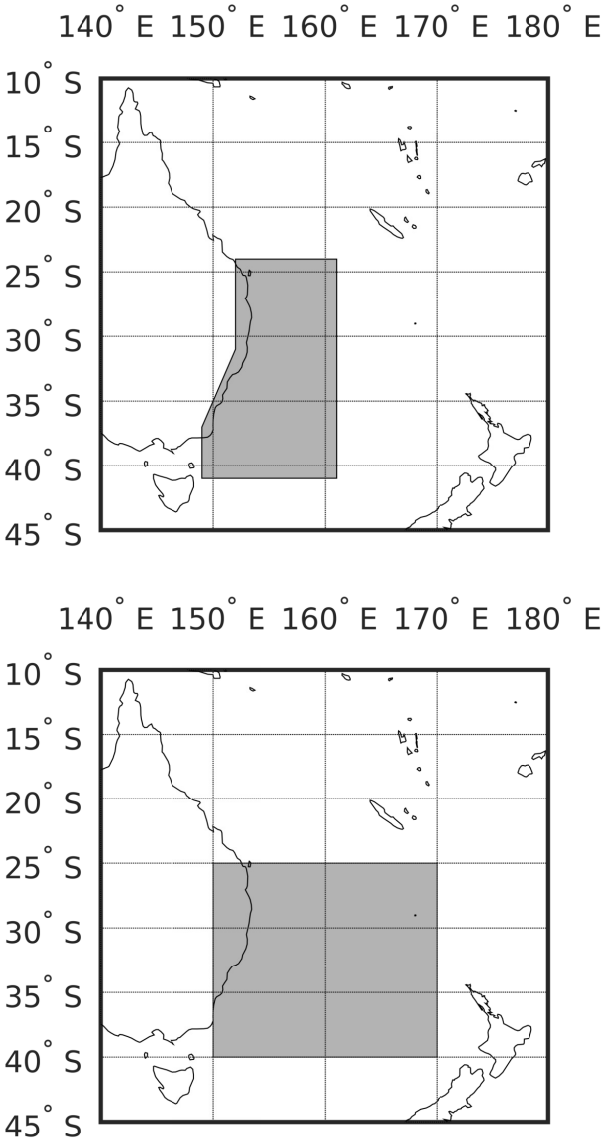

921 FIG. 3. Top: ECL tracking region used in the detection algorithm. Bottom: domain used for the computation
922 of cyclone energetics parameters.

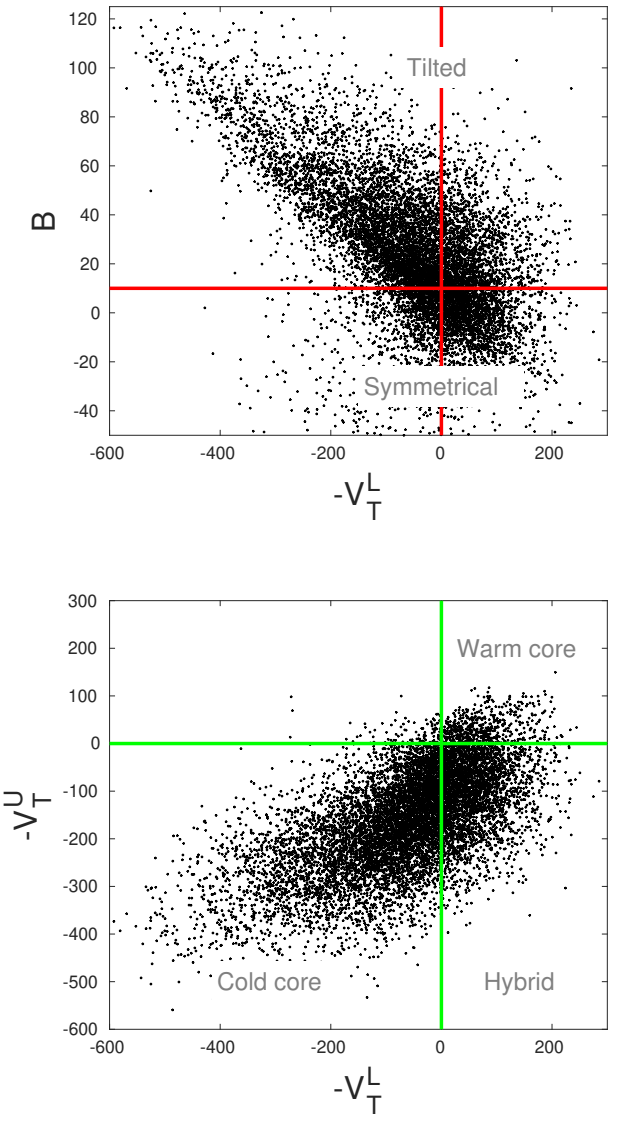

FIG. 4. Cyclone phase space diagrams for all cyclones detected in ERA-Interim in the ECL region for the period 1979-2016. Each dot corresponds to a single cyclone instance detected in a 6-hourly reanalysis time step.

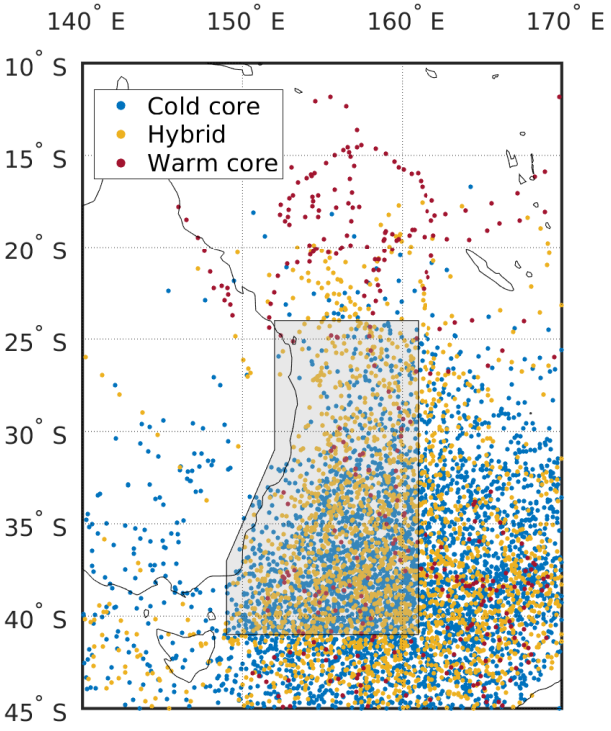

FIG. 5. Map of storm occurrence according to the cyclone phase space classification for all cyclones detected in ERA-Interim in the ECL region for the period 1979-2016. Each dot corresponds to a single cyclone instance detected in a 6-hourly reanalysis time step. Blue dots are cold core cyclones, yellow dots are hybrid cyclones, and red dots are warm core cyclones.

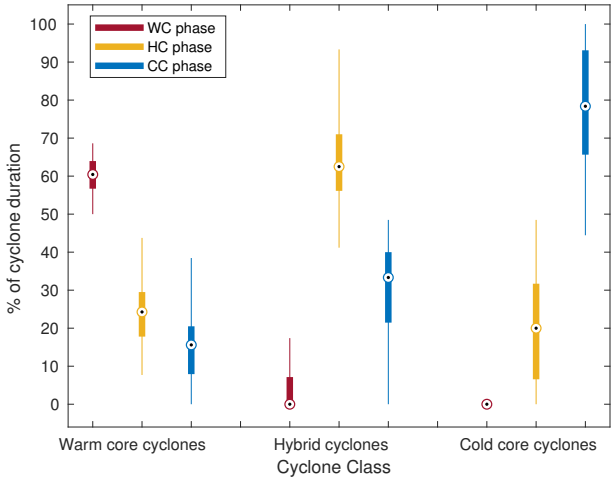

FIG. 6. Cyclone phase transition box plot. For each cyclone class (as indicated on the x axis, the plot indicates the likelihood of transitioning to different classes vs staying in the prevailing class by representing the climatological fraction of the total lifetime the cyclones are found in different phases (as indicated by the colors).

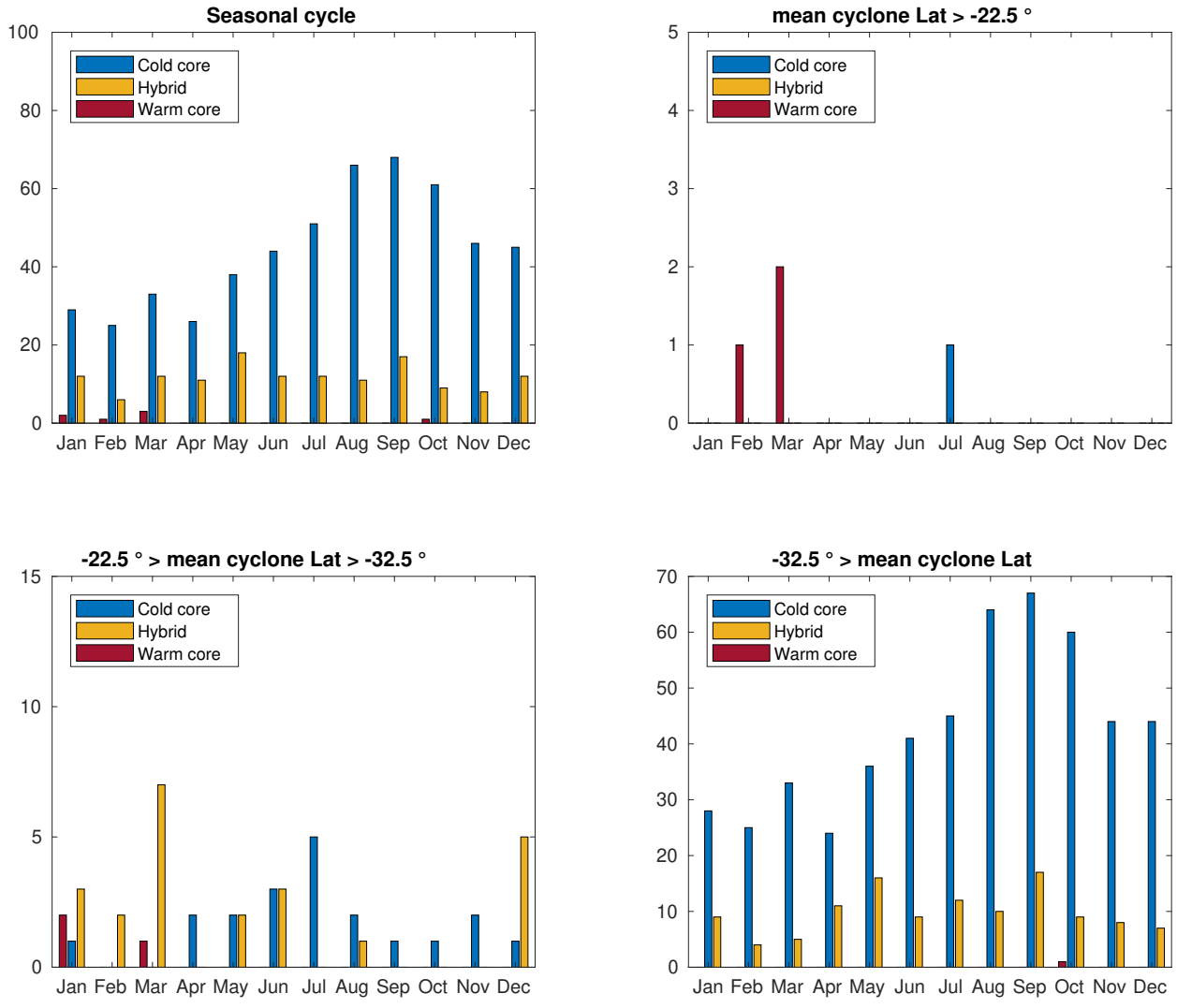

FIG. 7. Seasonal cycle for all cyclones detected in ERA-Interim for the period 1979-2016, according to their class and average latitude. Top left panel: seasonal cycle off all cyclones. Top right panel: cyclones with a mean latitude northwards of 22.5° S. Bottom left panel: cyclones with a mean latitude southward of 22.5° S and northward of 32.5° S. Bottom right panel: cyclones with a mean latitude southwards of 32.5° S.

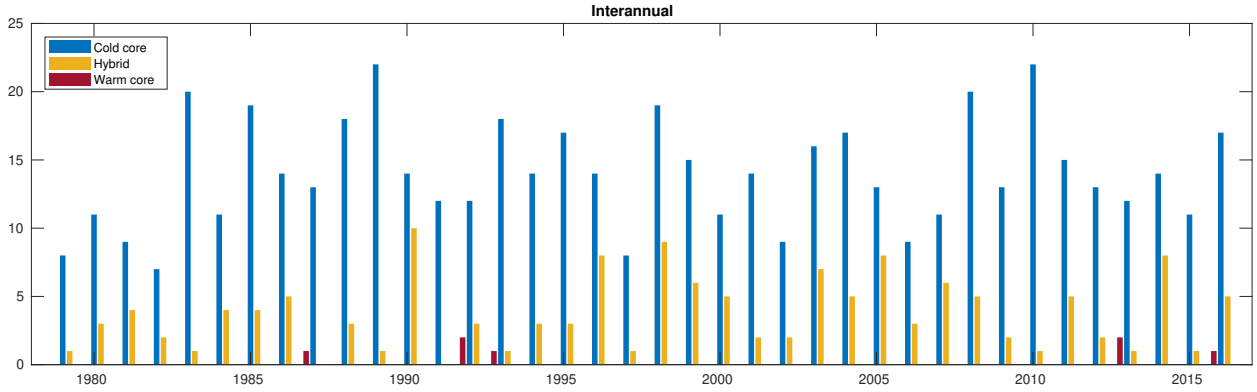

FIG. 8. Interannual time series of all cyclones detected in ERA-Interim in the ECL region for the period 1979-2016, according to the cyclone phase space classification.

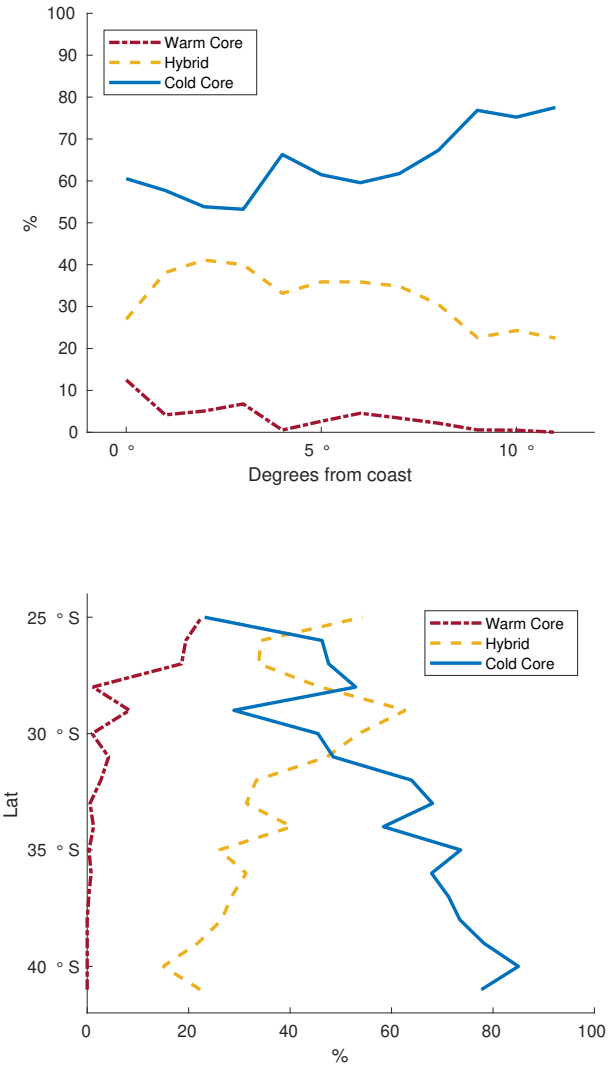

FIG. 9. Top panels: fractional frequency of each class of cyclones with respect to the total number of cyclones in each $1^\circ \times 1^\circ$ lat-lon box within the ECL region. a): warm core cyclones. b): hybrid cyclones. c): cold core cyclones. Bottom panels: zonally and meridionally averaged (within the ECL region) fractional frequency of each class of cyclones with respect to the total number of cyclones. d): zonal mean fractional frequency as a function of Latitude. e): meridional mean fractional frequency as a function of the distance from the Australian coast.

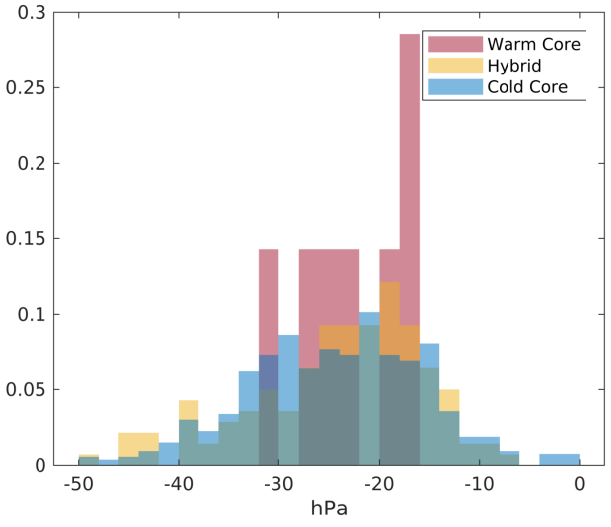

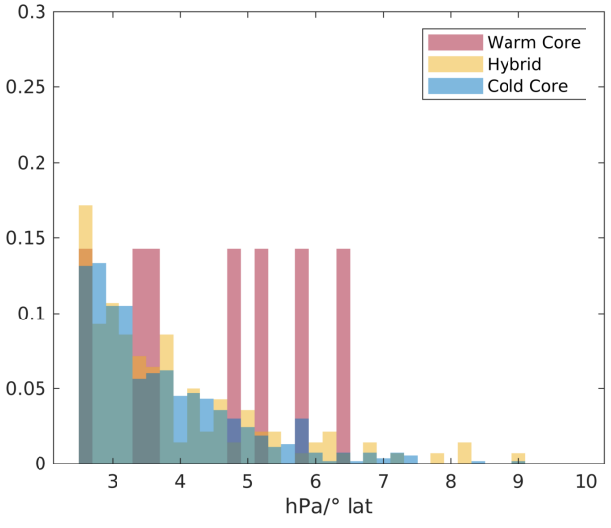

FIG. 10. Normalized histograms of different pressure-based metrics of intensity for all cyclones detected in ERA-Interim in the ECL region for the period 1979-2016. Top: lowest values of mean sea level pressure anomalies during the cyclone lifetime. Bottom: largest value of mean sea level pressure Laplacian during the cyclone lifetime.

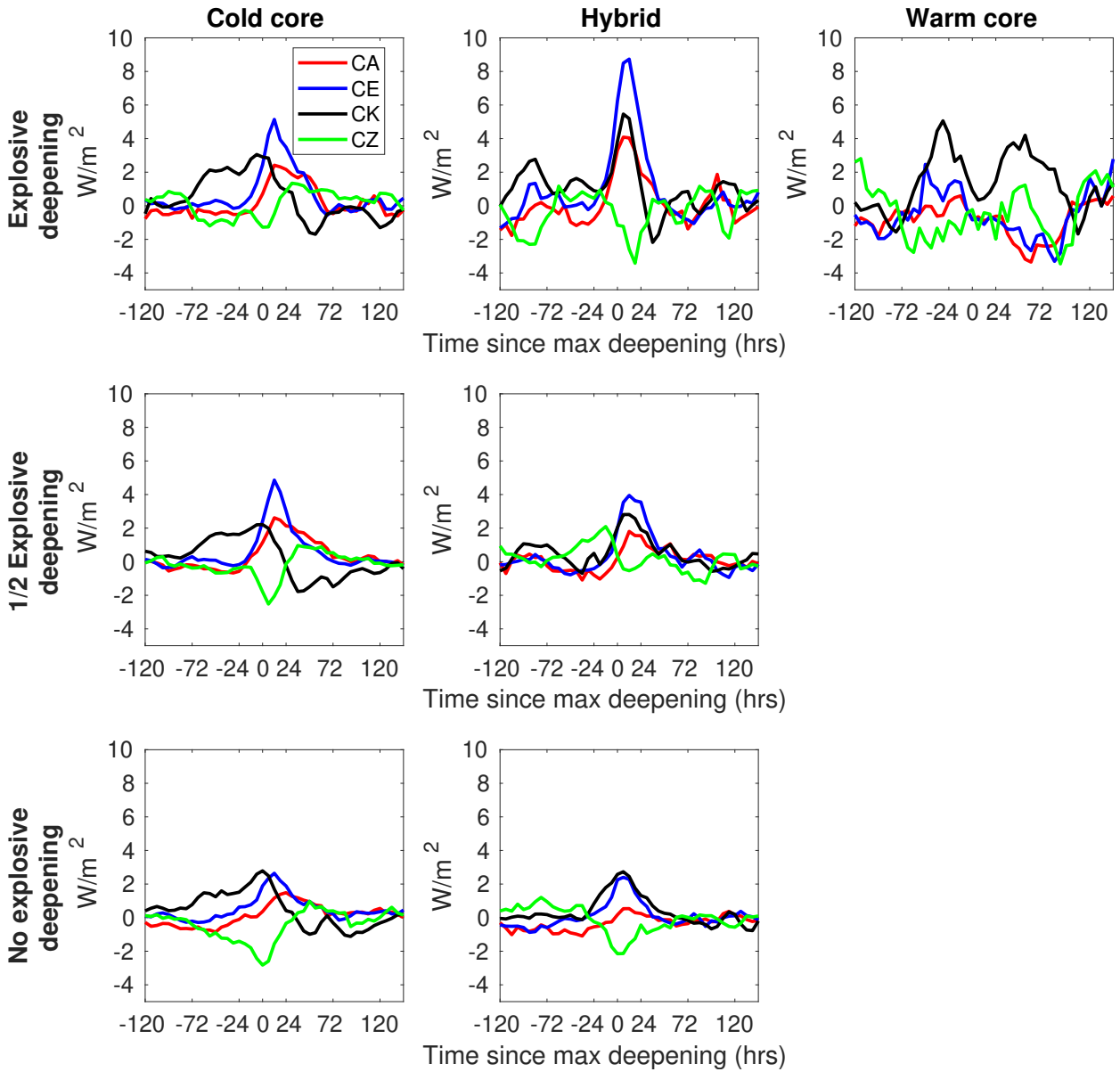

948 FIG. 11. Composites time series of the anomalies of the conversion terms in the energy cycle for different
949 types of cyclones detected in ERA-Interim for the period 1979-2016. Left column: cold core cyclones. Middle
950 column: hybrid cyclones. Right column: warm core cyclones. First row: explosively deepening cyclones. Sec-
951 ond row: cyclones with half explosive deepening. Last row: cyclones with no explosive deepening. Bomb and
952 half bomb cyclones are identified according to the original explosive intensification criterion, with a threshold
953 of respectively 24 hPa /24 hr and 12 hPa/24 hr.

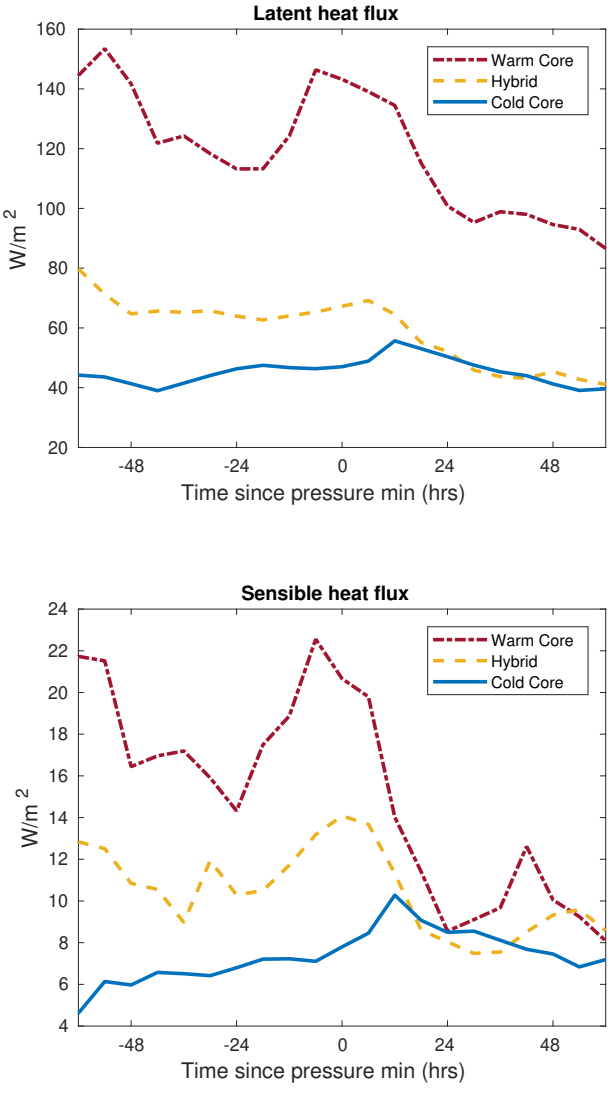

954 FIG. 12. Composites of surface fluxes for different types of cyclones detected in ERA-Interim for the period
955 1979-2016. Top: time series of latent heat flux. Bottom: time series of sensible heat flux. For each event in the
956 composite, the time step corresponding to the cyclone lifetime minimum sea level pressure is assigned the time
957 zero in the time series